3D Model-Based Tree Measurement from High-Resolution Aerial Imagery

P. Gong, Y. Sheng, and G.S. Biging

Abstract

This paper introduces a 3D model-based tree interpreter, a semi-automatic method for tree measurement from high-resolution aerial images. It emphasizes the extraction of the 3D geometric information such as tree location, tree height, crown depth (or crown height), crown radius, and surface curvature. First, trees are modeled as 3D hemi-ellipsoids with the following parameters: tree-top coordinates, trunk base height, crown depth, crown radius, and crown surface curvature. This model-based approach turns a tree interpretation task into a problem of optimal tree model determination. Multi-angular images are used to determine the optimal tree model for each tree. Tree tops in each image of a stereo pair are identified interactively with the epipolar constraint, and the 3D geometry of trees can be determined automatically. With such a semi-automatic scheme, efficiency and reliability of 3D tree measurements are achieved by taking advantages of both the operator's interpretation skills and the machine's computation. This paper mainly deals with conifers. The method was tested with a closed conifer stand on 1:2,400-scale photographs. An overall accuracy of 94 percent and 90 percent was obtained for tree height and crown radius measurements, respectively.

Introduction

Satellite remote sensing is a major tool for monitoring forest land over a large region (Sader, 1988; Sedykh, 1995), while field-based inventory with the assistance of aerial photography is dominant in forest data collection (Brandtberg, 1997). Forest photointerpretation in the past, however, focused on small- to medium-scale photos, and aerial photographic applications are largely stand-based. One major use of aerial photographs in forestry is to classify forest stands into land types (Aldrich, 1953), forest types (Sandor, 1955), and classes of stand volume (Aldrich and Norick, 1969).

Photointerpretation is a procedure involving the viewing and examination of stereopairs of aerial photographs by an interpreter with various optical instruments such as stereoscopes or stereoplotters. For forest inventory, the interpreter traces forest stand boundaries on the photos and determines the properties of the stand. In the digital era, a necessary follow-up step is to digitize the interpreted map into a computer to be managed in a geographic information system (GIS). On-screen digitization is an alternative to the hardcopy approach. Compared to the "hardcopy" approach, the "on-screen" approach has the following advantages: first, the images can be clearly viewed through image zooming and enhancement; second, and more importantly, the boundaries are already in digital forms so that no subsequent digitization is necessary.

Individual trees are only visible on large-scale aerial photographs. However, large-scale aerial photographs have not been widely used in forest inventory. The Canadian Forest Management Institute conducted several tests in the 1970s to evaluate the potential of large-scale photographs in deriving forest parameters for individual trees (Aldred and Kippen, 1967; Brun, 1972; Aldred and Sayn-Wittgenstein, 1972; Bonnor, 1977; Aldred and Lowe, 1978; Sayn-Wittgenstein, 1978; Sayn-Wittgenstein *et al.*, 1978). The photographs contained a great amount of detail with the scales ranging from 1:800 to 1:4000, and the methods used were manual photointerpretation.

With the increasing availability of large-scale photographs and high-resolution imagery, a new round of research on computer-based photointerpretation of trees was recently initiated (Gougeon, 1992; Gougeon, 1995; Pollock, 1996; Larsen, 1997; Gong *et al.*, 1999; Gong *et al.*, 2000). The key procedure here would be tracing crown boundaries for individual trees. This is a labor-intensive and time-consuming task. Some additional problems are foreseeable. The relief displacement caused by crown morphology becomes a serious disturbing factor when the photo scale is large because of the perspective nature of photographs. This may cause incompatibility between the interpreted map and other orthographic data in a GIS. The interpretation results can be very different when photographs are taken from different directions of the same area.

The above interpretation approach can be considered as a two-dimensional photointerpretation technique, which sometimes involves only monocular photos, and treats trees in a photo as 2D flat objects. With 2D photointerpretation techniques, we may get reliable information on species and number of trees, but not for parameters related to tree geometry such as crown size, crown closure, and tree locations, because the 3D morphology of trees is ignored. The perspective projection and crown morphology play a crucial role in tree interpretation. For tree interpretation on large-scale photographs, it is desirable to interpret trees from multi-angular photos based on 3D measurements.

Quantitative tree interpretation from aerial photographs is hardly possible for conventional interpretation on hardcopy photographs, and difficult even with stereoplotters. Computer-assisted approaches seem to be the only possible solution. Computer-based 3D aerial photointerpretation is currently dedicated to man-made objects (e.g., roads and buildings). Although efforts have been made to conduct automatic reconstruction of man-made objects (Kim and Muller, 1996; Lammi,

P. Gong is with the International Institute for Earth System Science, Nanjing University, Nanjing, China, 210093 and CAMFER, 151 Hilgard Hall, University of California, Berkeley, CA 94720-3110 (gong@nature.berkeley.edu).

Y. Sheng and G.S. Biging are with CAMFER, 151 Hilgard Hall, University of California, Berkeley, CA 94720-3110.

Photogrammetric Engineering & Remote Sensing
Vol. 68, No. 11, November 2002, pp. 1203–1212.

0099-1112/02/6811–1203$3.00/0

1997; Kim and Muller, 1998), it is still an unresolved issue (Gruen and Li, 1997), and operator-assisted semi-automatic approaches are emerging as the dominant trend (Agouris, 1997). Sahar and Krupnik (1999) extracted building outlines from bi-ocular images with a semiautomatic approach. Buildings are detected interactively, and 3D building outlines are extracted automatically. Gruen (1998) developed a system called TOBAGO (Topology Builder for the Automated Generation of Objects from 3D Point Clouds) to generate 3D models of buildings. TOBAGO is also a semi-automatic system, where the operator measures in the stereo mode, with an analytical plotter or a digital photogrammetric station, unstructured point clouds of building roofs. Buildings are then reconstructed by an automated procedure fitting 3D generic models of roofs to the point clouds. In concept, semi-automatic building reconstruction algorithms contain two steps: first, to interactively identify building features, e.g., building corners and edges, and then to automatically construct building models.

Tree interpretation is more challenging than building reconstruction because trees are semi-transparent 3D natural objects with large variations in appearance; there are few definite features of trees; and occlusions caused by trees are common in an image of forests. The purpose of this paper is to develop a low-cost computer-based interactive system to facilitate efficient 3D interpretation of trees. Such a system can work on any computer with no special hardware requirement so that it can be easily adapted to any application system.

Design of a 3D Model-Based Tree Interpreter

The following tree parameters are usually recorded in ground-based forest inventories: tree species, tree height, diameter at breast height (DBH), crown radii, and crown depth. Because tree trunks are normally invisible from aerial views, DBH cannot be measured directly from aerial photos but is obtained from other parameters (Biging *et al.*, 1995). A 3D tree interpreter should provide the following crown-related parameters: tree height, crown radius, crown depth, and higher order crown surface descriptions such as surface curvature.

It is possible to implement 3D interpretation in an efficient way. Because trees are 3D objects with both vertical and horizontal dimensions, we developed a model-based approach. We first use a 3D geometric tree model to describe a tree. Thus, we turn the tree interpretation task into an optimal tree model determination problem. We determine the optimal model by superimposing the model-synthesized tree outline on top of the images, and adjusting the tree model parameters until the best match of the outline on the images is reached. The parameters of the optimal model, which best describes a tree, are the measurements of the tree. The tree model parameters are determined in the object space; therefore, the tedious boundary-tracing task on the images can be avoided.

3D Geometric Tree Model

We adopted geometric models in tree modeling for their simplicity in parameterization. Horn proposed the following equation as a general model for the two-dimensional vertical profile of a crown envelope (Horn, 1971): i.e., $(z^{cc}/ch^{cc}) + (y^{cc}/cr^{cc}) = 1$, where ch and cr are the vertical and horizontal dimensions of a crown, respectively, and cc is a positive adjusting coefficient for crown curvature. When $cc = 1$, the curve is a straight line, $cc < 1$ indicates an increasingly upwards concave curve, while $cc > 1$ represents an increasingly downwards concave curve. Pollock extended Horn's formula into three dimensions, and modeled a crown envelope with a generalized ellipsoid: i.e., $(z^{cc}/ch^{cc}) + ((x^2 + y^2)^{cc/2})/cr^{cc} = 1$ (Pollock, 1996). For the purpose of applying the crown model to 3D crown surface reconstruction, Sheng *et al.* (2001) extended it to a tree model by adding the tree-top location and trunk base height. As illustrated in Figure 1a, this tree model is

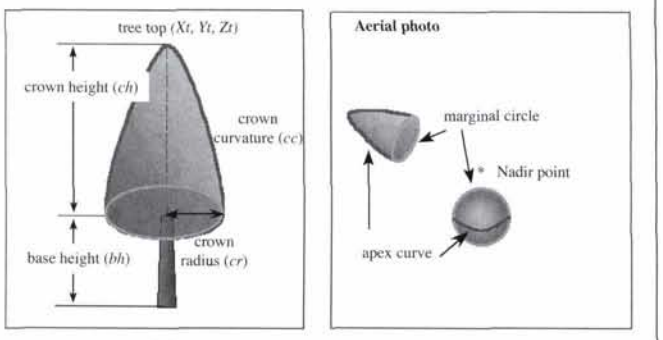

Figure 1. Illustration of a tree model and tree silhouette on a photograph. (a) A 3D geometric tree model consists of three location parameters (*Xt*, *Yt*, *Zt*), and four parameters of tree dimension: truck base height (*bh*), crown depth (or crown height, *ch*), crown radius (*cr*), and crown surface curvature (*cc*). (b) The silhouette of a tree on a photograph is the apex curve and the marginal circle of the tree projected on the photograph.

described by three location parameters: i.e., ground coordinates of the tree top (*Xt*, *Yt*, *Zt*); and four parameters on tree dimensions: i.e., trunk base height (*bh*), crown depth (*ch*), crown radius (*cr*), and an adjusting coefficient for crown curvature (*cc*). Once these seven parameters are known, the tree model is fixed and the ground coordinates (X, Y, Z) of any point on the crown surface can be modeled by

$$\frac{(Z + ch - Zt)^{cc}}{ch^{cc}} + \frac{((X - Xt)^2 + (Y - Yt)^2)^{cc/2}}{cr^{cc}} = 1 \qquad (1)$$

where $Zt - ch \leq Z \leq Zt$.

When tree height is known, as discussed below, trunk base height is dependent on crown depth. Crown depth, crown radius, and crown curvature are the three fundamental parameters to tree morphology. These three parameters form a 3D object space of a tree. We only include fundamental parameters in our model in order to make the model concise and the optimal tree model determination simple. Although the shapes of trees in the natural environment are too diverse to be described using such a simple model, we make the simplifying assumptions that trees are symmetric and are not leaning. These assumptions hold for most conifer trees in natural stands.

These dimensional parameters are related to each other, and this relationship varies among different species. For example, discrepancies can be found between conifers and hardwoods. The tree dimension configuration used in this paper for conifers and hardwoods is listed in Table 1. For conifers, crown

TABLE 1. TYPICAL PARAMETER SETTINGS FOR TREE MEASUREMENT

Parameters		Conifer	Hardwood
Crown depth (m)	Typical	25	7
	Min	15	2.5
	Max	40	15
Crown radius (m)	Typical	5	7
	Min	3	2.5
	Max	8	15
Crown curvature	Typical	1.2	2.0
	Min	1.0	1.5
	Max	1.8	2.5
Crown depth/tree height		0.85	0.6
Crown radius/crown depth		0.2	1.0

depth ranges from 15 m to 40 m, while crown radius is between 3 m and 8 m, and curvature is between 1.0 and 1.8. A typical setting for the ratio of crown depth to tree height is 0.85, and the ratio of crown radius to crown depth is set to 0.2.

Photo Model

Multi-angular imagery is needed for 3D interpretation of trees. The top of a conifer usually is not quite recognizable on a photograph when it is viewed directly from above. Off-nadir views are more informative to tree tops, while the nadir view is informative to crown closure due to fewer occlusions. Therefore, three images, i.e., one nadir view and two off-nadir views, are necessary to determine an optimal tree model. Because tree interpretation is implemented in the object space, photo-orientation parameters need to be known to transfer photo coordinates and ground coordinates back and forth. Orientation parameters of each image can be determined through photogrammetric orientation procedures. The three images (labeled as #2, #1, and #0 for the left, middle, and right images in this paper, respectively) resampled to the epipolar geometry form three stereo pairs. The pair formed by the two off-nadir images (i.e., images #2 and #0) is used as the primary pair in tree interpretation discussed here.

3D Tree Interpretation Scheme

Three-dimensional tree interpretation can be done with a computer at various levels of automation: interactively, semi-automatically, and fully automatically. The degree of possible automation depends on image quality and the complexity of a forest such as stand density, stand structures, tree forms, and contrast between trees and their background.

The tree interpretation task consists of tree-top detection, crown delineation, crown geometric reconstruction, and species identification. Existing computer-based tree-top location methods (Larsen, 1997) work under specific circumstances while tree delineation methods (Gougeon, 1995; Pollock, 1996) are automated versions of 2D interpretation with a monocular photo. They are not able to cope with complicated forest scenes. The difficulties of fully automatic techniques include the lack of definite image features of trees, problems of tree-top identification and tree dimension determination, occlusions, and varying algorithm performance with image complexity.

Because automatic methods for tree interpretation are not readily available, practical systems are desirable. We adopt a semi-automatic approach to 3D tree interpretation, which efficiently combines the advantages of both operators and computers to produce reliable 3D tree information. With such a system, we can increase the efficiency of manual interpretation as well as the reliability of automatic reconstruction of tree models.

The 3D tree-interpretation procedure includes the determination of the elevation of the tree base, the measurement of the coordinates (Xt, Yt, Zt) of a tree top, the initialization of a tree model with typical settings, the determination of the optimal tree model, and the validation of the tree model (Figure 2). The tree-top is picked up interactively on bi-ocular images. The validation is achieved by superimposing the synthesized tree outline on the images with photo-orientation parameters.

Tree-Base Elevation Determination

To determine the coordinates of any point in the object space, its image coordinates in the two images (the left and the right) of a stereo pair need to be measured. After the operator interactively picks up the conjugate points of a tree base on the left and right images of the primary pair, the system calculates the elevation of the tree base. A tree-base elevation may be shared among neighboring trees. Usually there is no need to measure the tree-base elevation for each individual tree.

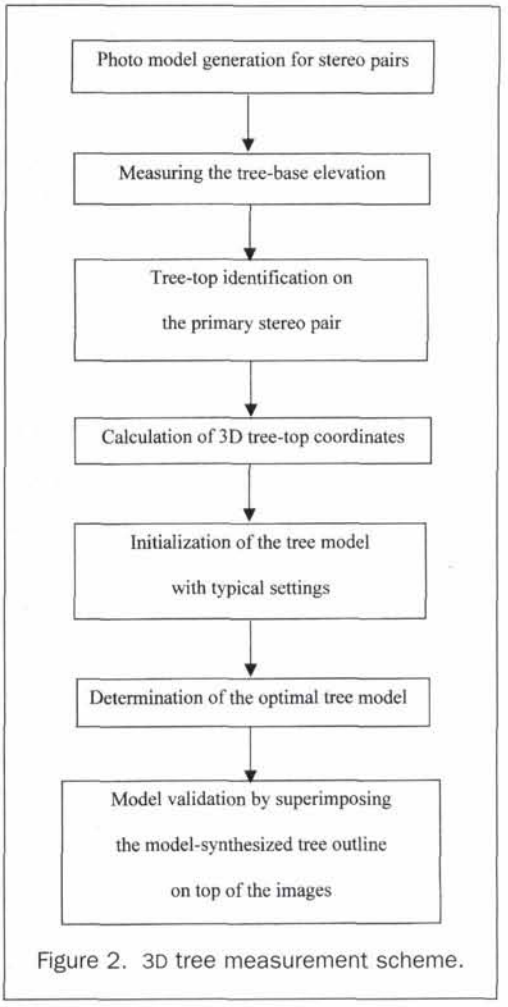

Figure 2. 3D tree measurement scheme.

Tree-Top Identification

Tree-top identification is a challenge to automation. As in tree-base elevation determination, the operator identifies the conjugate points of a tree top on the bi-ocular images, and the system calculates its 3D coordinates.

Tree Model Initialization

Tree height can be determined by subtracting the tree-base elevation from the Z coordinate of the tree top. Once the tree height is fixed, three parameters need to be determined: crown depth, crown radius, and surface curvature. Applying the typical parameter settings of tree morphology in Table 1, we can have a rough estimation of tree shape, which serves as the initial tree model. For example, suppose the top of a conifer tree is measured (Xt = 4366.86 m, Yt = 4056.79 m, and Zt = 50.90 m) and the tree base is at an elevation of 25.18 m, then the tree height is calculated as 25.72 m. Other tree parameters can be determined from the conifer column in Table 1: ch = 21.86 m, cr = 4.37 m, and cc = 1.2. These are the parameters of the initial model.

Tree Silhouette Computation

Overlaying the outline of the synthesized tree on top of the images helps to determine the optimal tree model. Gagnon *et al.* (1993) used circles superimposed on tree tops to measure conifer crown radius. Theoretically, this only works for trees around the nadir point of a photograph. The photographic geometry and the 3D crown shape play crucial roles in determining the appearance of a tree on a photo. As the position

of a conifer tree becomes farther away from the nadir point of the photograph, the top of the tree radiates away from it. As a result, a tree appears circular around the nadir point, and triangular or conic away from it.

The outline of a tree on a photograph is the silhouette of the 3D tree. A silhouette is the intersection curve of the tree surface and the surface constructed by the view rays. We separate the silhouette curve into two parts: the horizontally marginal circle and the vertical apex curve (Figure 1b). The marginal circle is easy to determine, but not the apex curve. It has to be determined through surface intersection.

The calculation of the intersection curve of two surfaces is a challenging task in computer graphics and mathematics (Ding and Davies, 1987; Takamura and Higuchiuchi, 1993). The curve is determined by the solution of non-linear equations, unless the two surfaces are planes. In our case, an analytical solution is impossible for the intersection of a generalized ellipsoid and another non-linear surface. By replacing the perspective view-rays with parallel ones, we simplify the non-linear surface intersection problem to that of a generalized ellipsoid and a plane. The solved curve is a reasonable approximation to the real silhouette curve because the camera, compared with tree dimension, is far from the tree. With the photo-orientation parameters, we can then project the silhouette curve to any of the images using the photogrammetric collinear equations.

Tree Parameter Adjustment

By overlaying the silhouette curve on the images, the operator can tell if the tree location and the dimensional parameters are acceptable. The operator can obtain appropriate parameters of the tree interactively by adjusting these parameters in the object space to make the silhouette match the tree edge on the images. It is also possible to determine these shape parameters automatically through the following steps: (1) specify a certain adjusting tolerance to each of these parameters, i.e., Δch, Δcr, Δcc to ch, cr, and cc; (2) construct tree models in the object space within the range of $[ch - \Delta ch, ch + \Delta ch]$ for ch, $[cr - \Delta cr, cr + \Delta cr]$ for cr, and $[cc - \Delta cc, cc + \Delta cc]$ for cc; (3) project the silhouette curve of each tree model to the image spaces; and (4) compute an edge indicator on the images around the projected silhouette curve. The tree model with the maximum edge indicator is selected as the optimal tree model. More than one image can be used in edge indicator computing, and the nadir-view image should always be included because this image is more informative regarding the horizontal parameters of a tree because trees are often partially occluded in off-nadir images.

Implementation and the User Interface

The 3D tree interpreter was developed in MATLAB® (MathWorks Inc., Version 5.2). As shown in Figure 3, the graphic user interface (GUI) of the interpreter consists of two major parts: the image windows and the control panel.

Three overlapping images form three stereo pairs. The three images are displayed in three separate image windows. The operator can read pixel value and coordinates, and zoom and roam the images through the mouse control. The three image windows are designed to display a stereo pair and the third image. The first window displays the left image in the pair, and the second displays the right one. These are the two active windows, where photogrammetric measurements of trees are taken. One of them is the primary image window and the other is the slave window. When making measurements from the stereo pair, the y coordinate in the slave image has to be identical to that in the primary image to keep the epipolar constraint. The third image window is for tree model validation by overlaying the tree silhouette curve on the corresponding tree.

The control panel is the core of the 3D tree interpreter. It is placed at the right hand side of the image windows. Its functions are organized into four groups: the Tree Info frame, the 3D Display frame, the Control frame, and the File frame.

Tree Info Frame

All tree model parameters are displayed in this frame, and are adjustable. The operator can specify the tree type as either conifer or hardwood. If the tree type is selected as conifer, all the parameters are set to typical conifer values. The operator can also sample the tree-base elevation in this frame. Many buttons in the Control frame collaborate with this frame and update its parameters.

3D Display Frame

With the tree parameters in the Tree Info frame, the operator can visualize the model-synthesized tree from the viewpoint of each photo to help in interpreting the tree. The 3D plot can be displayed using a wire-frame model or a Lambertian shading model.

Control Frame

The Control frame consists of many buttons for different functions.

- The Primary Pair list: The operator can select one of the three stereo pairs in this list as the primary stereo pair. The primary pair by default is the one formed by the two off-nadir images and this pair is treated as the working image pair. Images #2, #0, and #1 are displayed in windows 1, 2, and 3, respectively, but the operator can switch it to other pairs.
- The Primary Image list switches the primary image between the two active images.
- The Zooming button enables image zooming and roaming activities.
- The Darken (B−), Brighten (B+), De-contrast (C−) and Contrast (C+) buttons enhance the images through linear enhancement.
- The Place_treetop button activates the mouse button for picking the conjugate tree-top points in the left and right images.
- The Take_treetop button calculates the 3D coordinates of the tree top, and updates the tree-top coordinate editboxes in the Tree Info frame. The system computes the tree height, and sets the tree dimension editboxes and scrollers.
- The Place_tree button calculates the silhouette curve of the tree model, and projects the silhouette over the top of all the three images. If the tree silhouette does not outline the tree in the images, the operator can drag the silhouette curve with the mouse to the appropriate location, then click the Update_treetop button to update the tree-top coordinates in the Tree Info frame. If the tree outline is not of the right size, the operator can adjust the three parameters of tree dimension in the Tree Info frame, then generate and re-project the new silhouette curve with new configurations by clicking the Place_tree button again.
- The Take_tree button: Once the tree outline fits the tree in the images, the optimal tree model has been determined. The operator can take the tree parameters and add this tree to the tree list in the File frame by clicking the Take_tree button.
- The Auto_model button automatically determines the optimal tree model by computing and comparing the edge indicator of the images around the synthesized tree outlines of all the possible tree models. Collaborating with this button, three radio buttons choose the images to be used in the edge indicator computation.

File Frame

The File frame maintains a tree list and is responsible for file input and output.

- The Tree list contains all the measured trees with their parameters. The operator can browse the trees, and select any tree of interest from the list for further examination. The selected tree will be highlighted in red on the image windows.

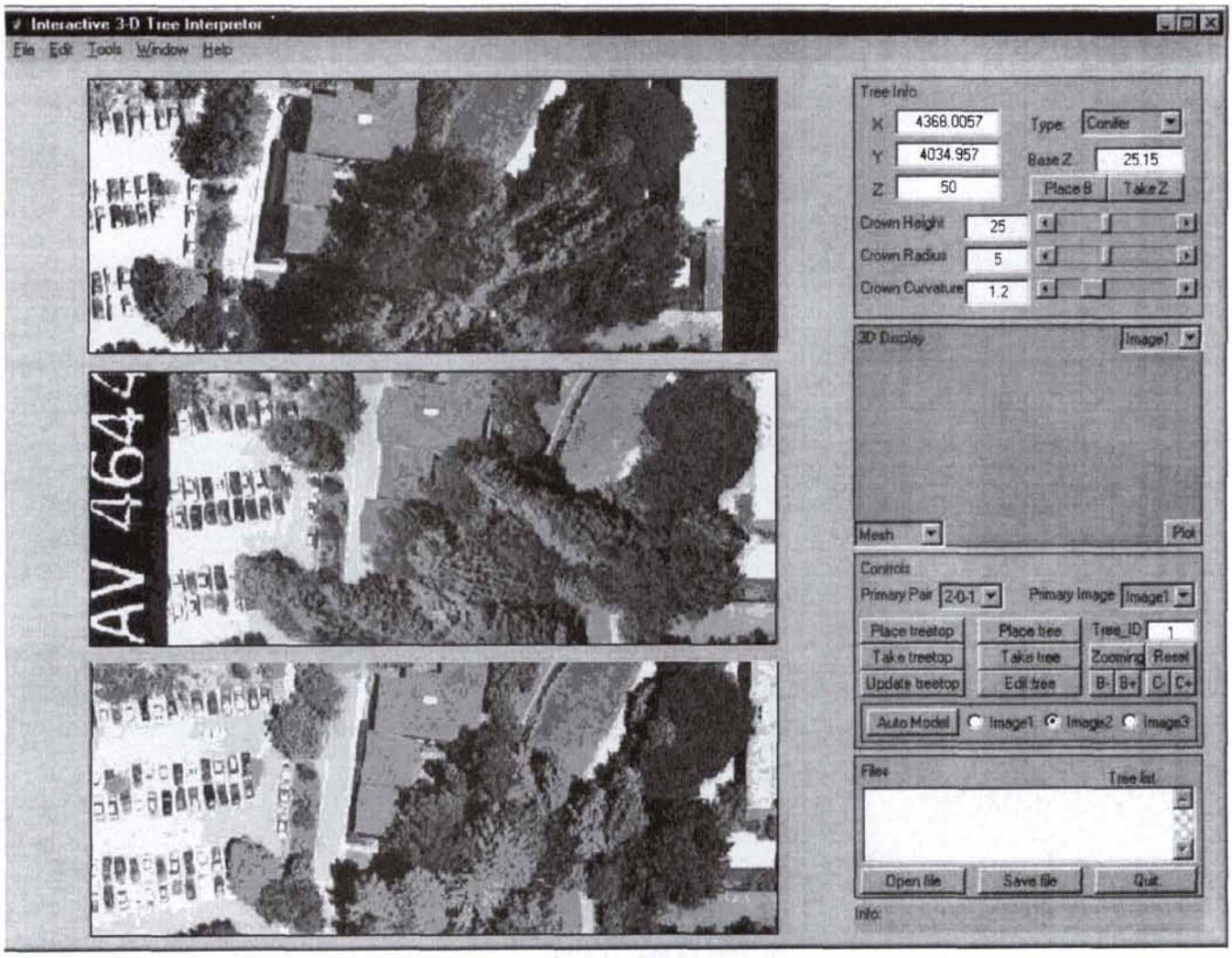

Figure 3. User interface of the 3D tree interpreter. The user interface consists of two parts: three image windows and the control panel.

- The Save_file button saves the tree list and the parameters to a tree data file.
- The Open_file button reads tree parameters from an existing tree data file, and projects the tree silhouettes on top of all the image windows.
- The Quit button prompts the operator to save the interpretation results, cleans the working environment, and quit the interpreter.

Interpretation of a Redwood Stand

The study site is a closed redwood stand at the Berkeley campus of the University of California (122.38°W, 37.62°N) with nearly 100 percent canopy coverage. Color aerial photographs were acquired on 23 May 1994 under clear sky conditions. The scale was 1:2,400. The camera focal length was 152.888 mm. Most of the stand is visible on the three overlapping photographs. These photos were scanned at 250 DPI (dots per inch), resulting in a pixel resolution of approximately 24 cm on the ground. The station location and camera attitude of the three photos were solved for through orientation procedures. The three photos form three stereo pairs: the 2-0 pair, the 2-1 pair, and the 1-0 pair. The photo model of the three stereo pairs is listed in Table 2. The 2-0 pair was used as the primary pair for tree-top identification because tree-tops are more recognizable on these off-nadir view images and the larger base line helps in precise determination of coordinates. The top-view image (image #1) was mainly used for tree crown size determination and validation.

TABLE 2. PHOTO MODELS OF THE STEREO PAIRS

Stereo Pair	Left Image		Right Image	
	Station Location (m)	Orientation (degree)	Station Location (m)	Orientation (degree)
Pair 2-0	4172.1	0.7953	4576.4	0.7953
	3999.7	0.0073	4003.5	0.0073
	399.1	0.5287	404.7	0.5287
Pair 2-1	4172.1	1.0996	4370.7	1.0996
	3999.7	0.0142	4002.3	0.0142
	399.1	0.7420	402.9	0.7420
Pair 1-0	4370.7	0.5015	4576.4	0.5015
	4002.3	0.0028	4003.5	0.0028
	402.9	0.3228	404.7	0.3228

(a)

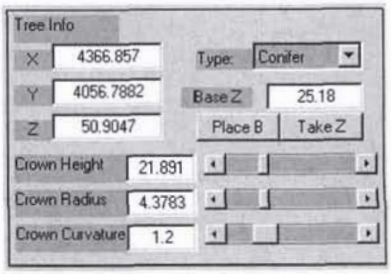

(b)

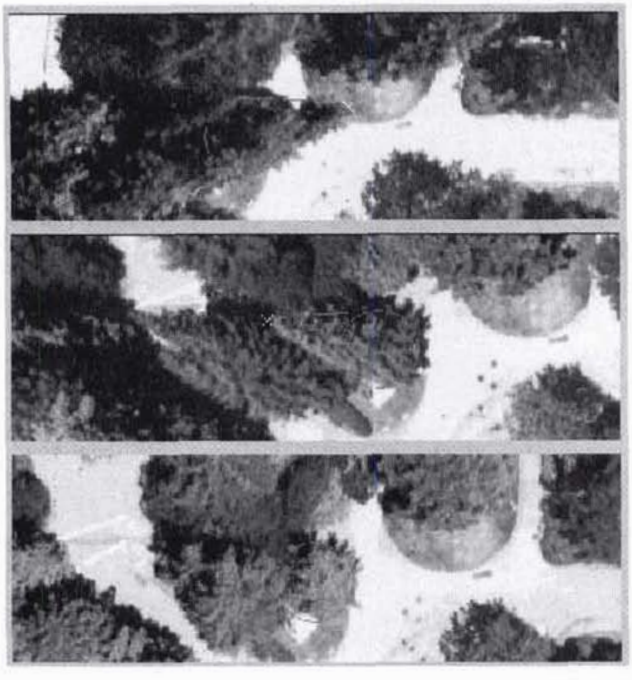

(c)

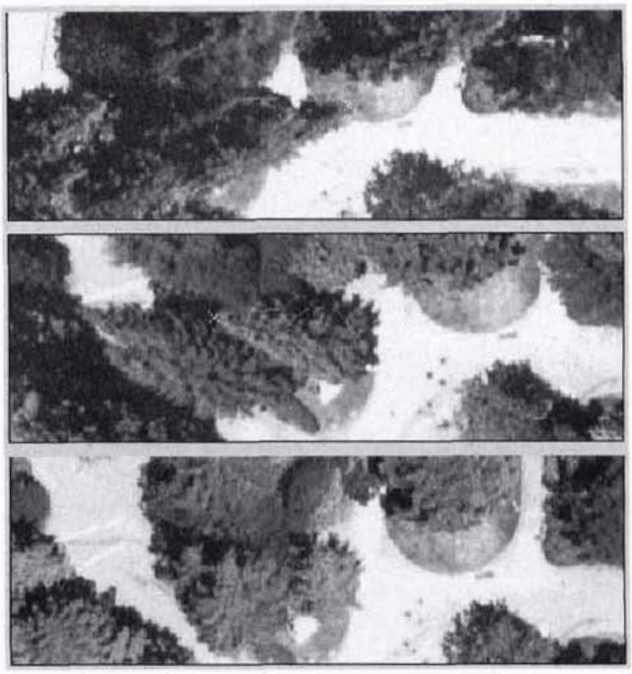

(d)

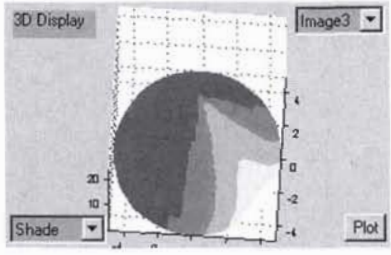

(e)

Figure 4. The interpretation procedure. (a) The tree-top picking step. (b) The tree model initialization step. (c) Superimposing the initial tree model (gray circles and cones at the central portions of the images) on top of the images. (d) Optimal model determination (gray circles and cones at the centers of images). (e) A 3D display of a model-synthesized tree.

We use here a tree as a tangible example to illustrate the proposed 3D tree interpretation scheme. This redwood tree is labeled as Tree #1. It was measured in the field with a height of 27.74 m and a crown radius of 4.92 m. First, the operator roams to center the image windows at this tree, zooms, and then enhances the images to display the tree as clearly as possible. The tree-base elevation is 25.18 m measured on the image. The tree top on the two active images (crosses in Figure 4a) can then be determined. Finally, the operator can click on the Take__treetop button to calculate the ground coordinates, estimate tree height, determine the initial tree model, and update the tree info frame (Figure 4b). The initial tree model is as follows: (Xt, Yt, Zt) = (4366.86 m, 4056.79 m, 50.90 m), tree height = 25.72 m, ch = 21.89 m, cr = 4.38 m, and cc = 1.2. So

far, the operator does not know if it is the optimal tree model for this tree. The Place_tree button can be clicked to overlay the synthesized tree outline on top of each image (Figure 4c). Now the operator can tell that this is not the optimal model because the outline does not match the tree edges on the images. Using the Auto_model tool and after necessary adjustments, the operator makes the tree outline fit the tree edge on the images (Figure 4d), and the optimal model is (Xt, Yt, Zt) = (4366.86 m, 4056.79 m, 50.90 m), tree height = 25.72 m, ch = 23.39 m, cr = 4.92 m, and cc = 1.1. The 3D plot from the viewpoint of the third image is shown in Figure 4e. The similarity between this 3D plot and the tree in the third image can be readily observed.

Sixty-two trees in this stand were measured using the same procedure. Figure 5 shows the top-view image overlaid with measured tree outlines. A visual inspection shows that the outlines in general match the image well. We also did a quantitative assessment of the photo measurements using ground measurements.

Field measurements were collected in October, 1999. Tree height, DBH, base height, and crown radii from four perpendicular directions were measured for 41 trees using clinometers and tapes. Three of the 41 trees measured were out of the area covered by these three images. Therefore, 38 trees were used for accuracy assessment. The interpreted tree parameters and the ground measurements are listed in Table 3 for comparison.

We compared the interpreted crown radius with the average of the four ground-based radius readings. The overall accuracy is estimated as 91 percent, and the mean absolute error is 0.37 m. Eighty-two percent of the trees have errors smaller than 0.5 m, and the crown radius interpretation is 85 percent accurate for 84 percent of the trees. We can see from Table 3 that the crown radius of irregular trees tends to be overestimated. This error is caused by the symmetric crown shape assumption used in our method. Additional parameters should be added to the tree model in the future to make it asymmetry-compliant.

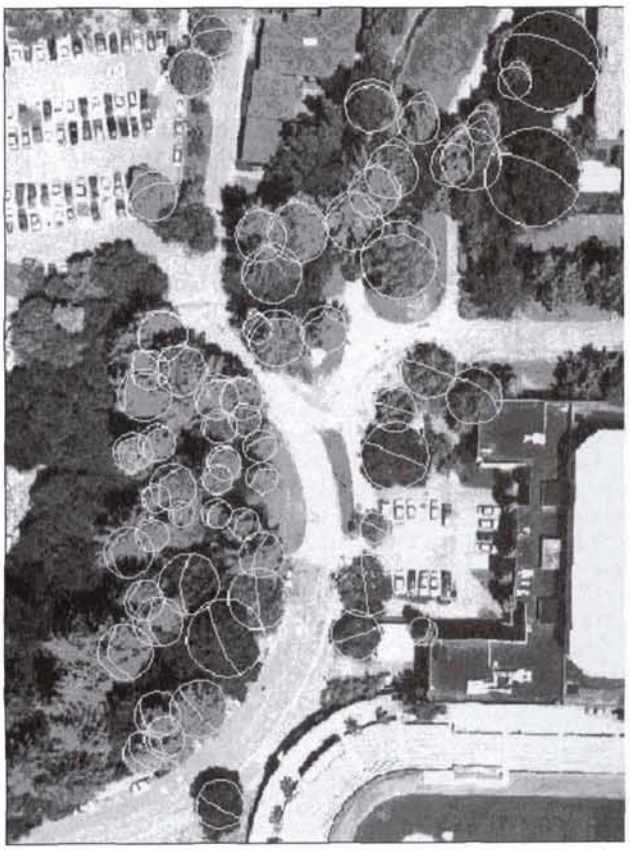

Figure 5. Interpreted tree outlines on top of the top-view image.

For tree height, the mean absolute error of tree height is 1.8 m, and the overall accuracy is estimated as 94 percent. The tree height error of 82 percent of the trees is less than 3 m, and 84 percent of the trees have a height estimation accuracy of better than 90 percent. The worst case in the 38 trees is Tree #2, whose height was overestimated by 6.8 m, equivalent to 24 percent of the ground-measured tree height. Though examined carefully, this tree top was not quite clear on the images.

Gagnon *et al.* (1993) reported that a high accuracy was achieved on tree height measurements for conifer plantation plots using softcopy photogrammetry. They claimed an accuracy of 48 cm could be reached using images scanned from 1:1,100-scale color photographs at 300 DPI when the tree-top coordinates are read as precisely as 0.3 pixel.

Theoretically, the object elevation h can be calculated from disparity using Equation 2: i.e.,

$$h = H - f\frac{B}{d} \tag{2}$$

where H is the camera height, B is the baseline, f is the camera focal length, and d is the disparity reading from the photos. Because the disparity reading is error-prone, the derived target height is subject to error. Take the derivative of d from Equation 2: i.e.,

$$\frac{\partial h}{\partial d} = \frac{\partial}{\partial d}\left(H - f \cdot \frac{B}{d}\right) = \frac{f \cdot B}{d^2} = \frac{(H-h)^2}{f \cdot B}. \tag{3}$$

The uncertainty in h due to error in disparity reading is

$$\partial h = \frac{(H-h)^2}{f \cdot B}\,\partial d. \tag{4}$$

The parameters of the primary stereo pair used in this paper are B = 404 m, H = 402 m, and f = 152.888 mm. For a tree top whose elevation is 50 m (the elevation of most tree tops in the redwood stand is around 50 m), i.e., h = 50 m, we can see that a one-pixel error in disparity reading may cause an error of only 0.2 m in tree-top elevation measurement with the photo configuration of the primary pair. Taking tree-base elevation measurement error into consideration, an accuracy of 0.4 m in tree height measurement is guaranteed if the disparity reading error is within one pixel. However, our overall accuracy of tree height measurement is about 1.8 m, which is much greater than the theoretical estimates. This can be explained by the fact that measurement accuracy is determined not only by the precision in disparity reading, but also by other factors such as image quality and stand complexity. Tree tops of a difficult stand are not very distinct on images of poor quality. Although we can read the disparity at sub-pixel precision, we may still get a poor tree height measurement because we may not pick up the right pixels for the tree top.

Interpretation efficiency also depends on many factors such as image quality, stand complexity, tree-top recognizability, and the operator's proficiency. For the redwood stand in this paper, a normal operator with our algorithm can interpret approximately 200 trees per day. The interpretation speed is expected to double for forest stands that are easier to interpret. This is much more efficient than field survey. It took two crew members four hours to measure the 41 trees in the field. This is

TABLE 3. INTERPRETATION RESULT VALIDATION WITH GROUND MEASUREMENTS

Tree ID	Species	Interpretation results							Field measurements (m)					Comparison			
		X (m)	Y (m)	Z (m)	CH(m)	CR(m)	CC	Zbase(m)	Height	R1*	R3	R5	R7	ΔH(m)+	ΔH%X	ΔR(m)	ΔR%
1	redwood	4366.86	4056.79	50.90	23.39	4.92	1.1	25.18	27.74	4.8	5.0	5.0	4.9	−2.01	−7.24	−0.01	−0.10
2	redwood	4382.29	4070.68	59.75	26.60	8.00	1.5	24.91	28.04	6.8	6.8	7.9	7.0	6.80	24.24	0.88	12.28
3	redwood	4372.81	4078.91	58.47	27.32	6.06	1.2	24.62	33.22	8.1	7.2	6.1	5.3	0.63	1.89	−0.61	−9.14
4	redwood	4376.97	4083.98	60.94	25.42	5.28	1.2	24.97	33.22	5.0	5.3	4.7	4.8	2.74	8.25	0.33	6.74
5	redwood	4355.69	4068.21	59.31	30.04	6.21	1.2	24.98	36.27	6.6	5.0	6.0	5.6	−1.93	−5.33	0.41	7.03
6	redwood	4353.48	4075.25	62.86	30.12	5.42	1.2	24.50	36.27	5.9	5.3	5.3	5.3	2.09	5.75	−0.03	−0.49
7	redwood	4361.11	4076.55	62.41	31.67	6.33	1.3	24.46	34.75	7.2	6.6	5.6	7.0	3.20	9.21	−0.27	−4.04
8	redwood	4356.91	4054.62	57.53	27.52	5.86	1.6	25.07	31.09	6.4	4.8	6.4	4.8	1.37	4.41	0.29	5.19
9	redwood	4352.92	4056.64	54.45	24.91	3.00	1.2	25.00	31.09	3.0	2.9	3.0	3.5	−1.64	−5.27	−0.10	−3.23
10	redwood	4353.50	4032.40	40.64	13.35	3.42	1.4	24.06	18.29	3.8	4.0	2.8	2.8	−1.71	−9.35	0.07	2.09
11	redwood	4354.15	4025.56	50.91	23.03	3.29	1	23.64	25.91	3.4	3.1	2.4	2.3	1.36	5.26	0.49	17.38
12	redwood	4346.24	4028.31	58.61	27.39	3.52	1.6	23.17	33.83	2.3	3.0	2.8	2.0	1.60	4.74	1.00	39.41
13	redwood	4345.05	4024.70	58.78	25.69	3.08	1.6	22.93	32.31	2.8	2.5	2.5	3.0	3.54	10.96	0.38	13.89
14	redwood	4350.22	4037.75	54.55	27.16	3.39	1.2	24.08	31.09	3.7	2.2	2.4	2.5	−0.62	−2.01	0.69	25.66
15	redwood	4349.46	4042.05	60.30	32.88	4.50	1.6	24.27	35.36	4.8	2.6	4.4	4.8	0.67	1.90	0.35	8.31
16	redwood	4344.54	4041.76	58.58	26.43	4.69	1.4	23.96	33.83	3.7	3.9	4.2	6.1	0.79	2.33	0.21	4.73
17	redwood	4345.08	4035.94	56.29	26.60	3.64	1.4	23.66	33.22	3.5	3.9	4.2	3.9	−0.60	−1.80	−0.23	−6.04
18	redwood	4337.19	4047.36	67.76	35.80	5.26	1.4	23.78	38.40	5.0	4.7	4.0	5.4	5.57	14.51	0.48	10.14
19	redwood	4333.18	4054.74	62.20	31.88	5.18	1.4	24.26	34.44	4.3	4.0	5.2	5.3	3.50	10.17	0.48	10.13
21	redwood	4330.76	4047.22	61.79	27.93	3.99	1.2	23.55	35.97	3.4	3.2	6.8	3.5	2.28	6.33	−0.24	−5.65
22	redwood	4329.48	4042.21	62.71	30.71	5.54	1.2	23.25	39.93	5.3	6.2	6.8	3.6	−0.48	−1.19	0.07	1.21
23	redwood	4329.18	4029.16	67.83	19.73	3.95	1.2	22.53	42.37	3.7	3.6	3.5	4.1	2.94	6.93	0.22	5.95
24	redwood	4332.99	4031.74	58.15	19.25	3.78	1.4	22.76	32.00	3.6	3.7	3.7	3.5	3.38	10.57	0.16	4.30
25	redwood	4332.04	4020.94	55.72	25.48	3.00	1.2	22.50	31.70	2.0	3.0	2.9	2.0	1.52	4.79	0.53	21.21
26	redwood	4335.38	4023.38	53.42	24.03	4.81	1.2	22.61	29.87	5.0	3.3	3.0	5.9	0.94	3.15	0.51	11.78
28	redwood	4337.46	4017.77	52.07	19.88	2.65	1.2	22.55	30.48	3.4	2.0	2.0	2.0	−0.96	−3.16	0.30	12.77
30	redwood	4331.12	4013.43	56.86	26.96	3.49	1.2	22.89	32.31	3.4	2.5	3.0	3.7	1.67	5.16	0.34	10.83
31	redwood	4326.30	4009.70	60.04	29.51	5.20	1.2	23.47	36.58	3.9	5.4	5.4	4.6	−0.01	−0.03	0.38	7.83
32	redwood	4350.32	4015.80	52.98	24.35	3.27	1.4	22.96	28.35	3.0	3.0	3.0	3.0	1.67	5.90	0.27	8.99
33	redwood	4344.65	4017.91	50.58	21.62	3.12	1.2	22.72	29.26	2.8	3.0	2.9	2.8	−1.40	−4.80	0.25	8.52
34	redwood	4354.04	4009.42	54.46	26.15	4.75	1.4	23.61	27.74	3.7	4.1	3.7	4.8	3.12	11.25	0.67	16.56
35	P. Mntry	4347.42	3992.16	56.51	19.65	8.00	1.8	24.00	30.48	11.2	6.1	2.0	8.0	2.03	6.65	1.18	17.22
36	redwood	4341.93	3977.42	41.97	6.11	6.00	2.1	23.86	18.90	6.3	6.0	5.0	5.4	−0.78	−4.15	0.33	5.81
37	redwood	4332.86	3975.86	54.36	24.00	4.80	1.6	23.78	29.26	5.5	4.2	4.1	4.9	1.32	4.53	0.13	2.68
38	redwood	4334.04	3970.62	51.42	25.64	4.33	1.4	23.87	26.52	5.2	4.8	3.6	3.5	1.03	3.90	0.05	1.24
39	redwood	4329.78	3967.74	45.51	17.31	4.46	1.4	23.68	21.34	5.2	4.5	4.5	3.0	0.49	2.31	0.16	3.74
40	oak	4346.03	3956.85	34.99	5.90	5.10	2	24.09	10.97	4.0	4.4	5.6	7.9	−0.08	−0.70	−0.37	−6.82
41	oak	4374.39	3992.80	32.68	3.77	5.17	2.3	24.86	7.32	6.4	6.0	5.8	4.5	0.51	6.95	−0.50	−8.83

*R1, R3, R5, and R7 are the ground crown radius readings from four perpendicular directions. The average of the four readings is used as the true value to evaluate the crown radius measured from the photos.
+ΔH is the difference between the photo-measured and the ground-measured tree heights. Similarly, ΔR is defined for crown radius.
XΔH% is the ratio of H to the ground tree height in percentage. Similarly, ΔR% is defined for crown radius.
SThe mean absolute error of tree height (or crown radius) is defined as the average of the absolute value of ΔH (or ΔR). The overall accuracy of tree height (or crown radius) is defined as 100 − averaged ΔH (or ΔR).

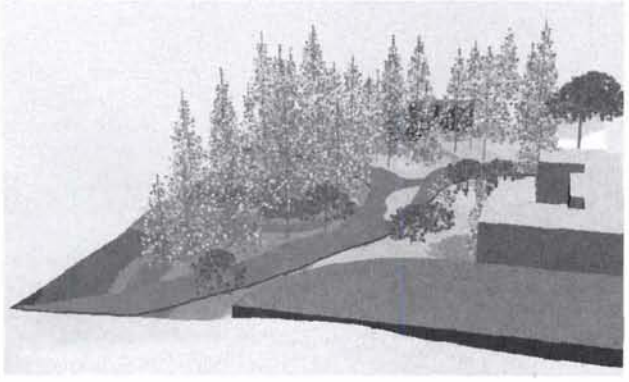

Figure 6. A snapshot of the 3D view.

a stand with flat topography. The tree interpreter is also more productive than stereoplotters. Kovats (1997) discussed the efficiency of using a stereoplotter to measure tree height from large-scale aerial photographs. Having the tree-base elevation predetermined, and with the assistance of ground stem maps, an operator can measure more than 300 trees per day. There, the operator made only one measurement for each tree, the coordinates of the tree top. In this effort, stereoplotters are only used to measure tree height, while our method outputs a wide range of tree measurements in an efficient way.

The interpretation results were imported into ArcView GIS. We developed a script to take the interpreted tree measurements and visualize the tree models with the ArcView 3D Analyst Extension. The 3D view looks quite realistic. A snapshot of the 3D view is illustrated in Figure 6.

Conclusions

We report preliminary results for model-based aerial photointerpretation of trees in this paper. A low-cost model-based 3D tree interpreter software system was developed. It can be easily transplanted to any system because no special hardware is required.

This interpreter system can produce many important tree measurements such as location, height, crown depth, crown radius, and crown surface curvature of trees. The outputs of the tree interpreter system are free of perspective distortion, and can be imported to a GIS to produce tree maps.

The 3D interpreter system works in an interactive manner but model matching and measurement are done automatically. Such a system combines a manual interpreter's reliability and the efficiency of a computer system. This integration is necessary and practical for tree interpretation in natural stands where automatic approaches usually fail.

Rather than directly tracing crown boundaries, our method synthesizes tree outlines from tree models and superimposes them on top of the images for model validation. In the 3D interpreter system design, we made use of image display techniques, triangular images and the epipolar constraint, and a user-friendly interface. All these improve the reliability and efficiency in tree interpretation. With this tree interpreter, an operator can measure approximately 200 trees in one day for quite complicated stands.

The accuracy of the measurements depends more on stand complexity, image quality, and the identifiability of tree tops on the images, rather than on how precise the operator can read the coordinates. As a consequence, the accuracy is expected to be higher for even-aged plantation plots, and lower for dense natural stands. For the closed redwood stand used in this paper, we have obtained acceptable tree measurements with an overall accuracy of 94 percent and 90 percent for tree height and crown radius, respectively. We expect to achieve better results at a higher interpretation speed for easier stands. The results also show that there is room for improving the performance of this approach by upgrading the tree model to a more sophisticated one.

In addition to measurements of tree parameters, these measurements can serve as initial conditions for further research such as tree pattern analysis, crown surface reconstruction, and orthographical tree image generation.

References

Agouris, P., 1997. Foreword to the 1997 Softcopy Photogrammetry Special Issue, *Photogrammetric Engineering & Remote Sensing*, 63(8):958.

Aldred, A.H., and F.W. Kippen, 1967. *Tree Measurements on Large-Scale Oblique Photos*, Information Report FMR-X-4, Forest Management Institute, Ottawa, Ontario, Canada, 14 p.

Aldred, A.H., and L. Sayn-Wittgenstein, 1972. *Tree Diameters and Volumes from Large-Scale Aerial Photographs*, Information Report FMR-X-40, Forest Management Institute, Ottawa, Ontario, Canada, 39 p.

Aldred, A.H., and J.J. Lowe, 1978. *Application of Large-Scale Photos to a Forest Inventory in Alberta*, Information Report FMR-X-107, Forest Management Institute, Ottawa, Ontario, Canada, 57 p.

Aldrich, R.C., 1953. Accuracy of land-use classification and area estimates using aerial photographs, *Journal of Forestry*, 51(1):12–15.

Aldrich, R.C., and N.X. Norick, 1969. *Stratifying Stand Volume on Non-Stereo Aerial Photos*, PSW-51, Pacific Southwest Forest and Range Experiment Station, Berkeley, California, 14 p.

Biging, G.S., M. Dobbertin, and E.C. Murphy, 1995. A test of airborne multispectral videography for assessing the accuracy of wildlife habitat maps, *Canadian Journal of Remote Sensing*, 21(3):357–366.

Bonnor, G.M., 1977. *Forest Inventories with Large-Scale Aerial Photographs: An Operational Trial in Nova Scotia*, Information Report FMR-X-96, Forest Management Institute, Ottawa, Ontario, Canada, 21 p.

Brandtberg, T., 1997. Towards Structure-based classification of tree crowns in high spatial resolution aerial images, *Scandinavian Journal of Forest Research*, 12(1):89–96.

Brun, R., 1972. *A New Stereotype Digitizer System for Measuring and Processing Tree Data from Large-Scale Aerial Photographs*, Information Report FMR-X-41, Forest Management Institute, Ottawa, Ontario, Canada, 35 p.

Ding, Q., and B.J. Davies, 1987. *Surface Engineering Geometry for Computer-Aided Design and Manufacture*, Ellis Horwood Limited, New York, N.Y., 340 p.

Gagnon, P.A., J.P. Agnard, and C. Nolette, 1993. Evaluation of a softcopy photogrammetry system for tree-plot measurements, *Canadian Journal of Forest Research*, 23:1781–1785.

Gong, P., Greg S. Biging, S.M. Lee, X. Mei, Y. Sheng, R. Pu, B. Xu, and K.-P. Schwarz, 1999. Photo-ecometrics for forest inventory, *Geographic Information Sciences*, 5(1):9–14.

Gong, P., G. Biging, and R. Standiford, 2000. The potential of digital surface model for hardwood rangeland monitoring, *Journal of Range Management*, 53:622–626.

Gougeon, F.A., 1992. Individual tree identification from high resolution MEIS images, *Proceedings of the International Forum on Airborne Multispectral Scanning for Forestry and Mapping*, 13–16 April, Quebec, Canada (Canadian Forest Service, Petawawa, Ontario, Canada), pp. 117–128.

———, 1995. Comparison of possible multispectral classification schemes for tree crowns individually delineated on high spatial resolution MEIS images, *Canadian Journal of Remote Sensing*, 21(1):1–9.

Gruen, A., 1998. TOBAGO—A semi-automated approach for the generation of 3D building models, *ISPRS Journal of Photogrammetry and Remote Sensing*, 53(2):108–118.

Gruen, A., and H. Li, 1997. Semi-automatic linear feature extraction by dynamic programming and LSB-snakes, *Photogrammetric Engineering & Remote Sensing*, 63(8):985–995.

Horn, H.S., 1971. *The Adaptive Geometry of Trees*, Princeton University Press, Princeton, New Jersey, 144 p.

Kim, T., and J.P. Muller, 1996. Automated urban area building extraction from high resolution stereo imagery, *Image and Vision Computing*, 14(2):115–130.

———, 1998. A technique for 3D building reconstruction, *Photogrammetric Engineering & Remote Sensing*, 64(9):923–930.

Kovats, M., 1997. A large-scale aerial photographic technique for measuring tree heights on long-term forest installations, *Photogrammetric Engineering & Remote Sensing*, 63(6):741–747.

Lammi, J., 1997. Automatic building extraction using a combination of spatial data and digital photogrammetry, *Proceedings, Integrating Photogrammetric Techniques with Scene Analysis and Machine Vision III*, 22 April (D. McKeown, C. McGlone, and O. Jamet, editors), SPIE, Orlando, Florida, pp. 223–230.

Larsen, M., 1997. Crown modeling to find tree top positions in aerial photographs, *Proceedings of the International Airborne Remote Sensing Conference and Exhibition*, 03 July, Copenhagen, Denmark, pp. 428–435.

Pollock, R.J., 1996. *The Automatic Recognition of Individual Trees in Aerial Images of Forests Based on a Synthetic Tree Crown Image Model*, Ph.D Thesis, University of British Columbia, Vancouver, B.C., Canada, 172 p.

Sader, S.A., 1988. Satellite digital image classification of forest change using three Landsat data sets, *Remote Sensing for Resource Inventory, Planning, and Monitoring*, American Society for Photogrammetry and Remote Sensing, Bethesda, Maryland, pp. 189–201.

Sahar, L., and A. Krupnik, 1999. Semiautomatic extraction of building outlines from large-scale aerial images, *Photogrammetric Engineering & Remote Sensing*, 65(4):459–465.

Sandor, J.A., 1955. *Forest Type Classification*, Alaska Region, U.S. Forest Service, Regional Forester's Office-Region 10, Juneau, Alaska, 24 p.

Sayn-Wittgenstein, L., 1978. *Recognition of Tree Species on Aerial Photographs*, Information Report FMR-X-118, Forest Management Institute, Ottawa, Ontario, Canada, 97p.

Sayn-Wittgenstein, L., R. De Milde, and C.J. Inglis, 1978. *Identification of Tropical Trees on Aerial Photographs*, Information Report FMR-

X-113, Forest Management Institute, Ottawa, Ontario, Canada, 33 p.

Sedykh, V.N., 1995. Using aerial photography and satellite imagery to monitor forest cover in western siberia, *Water, Air and Soil Pollution*, 82(1–2):499–507.

Sheng, Y., P. Gong, and G.S. Biging, 2001. Model-based conifer crown surface reconstruction from high-resolution aerial images, *Photogrammetric Engineering & Remote Sensing*, 67(8):957–965.

Takamura, T., and S. Higuchiuchi, 1993. Intersection calculations, *3D CAD Principles and Applications*, (H. Toriya and H. Chiyokura, editors), Springer-Verlag, New York, N.Y., pp. 139–164.

(Received 03 August 2000; accepted 12 February 2002)